

Whispering-gallery-mode barcode-based broadband sub-femtometer-resolution spectroscopy with an electro-optic frequency comb

Bingxin Xu,^{†‡} Yangyang Wan,[†] Xinyu Fan,^{*} and Zuyuan He

Shanghai Jiao Tong University, State Key Laboratory of Advanced Optical Communication Systems and Networks,
Department of Electronic Engineering, Shanghai, China

Abstract. Spectroscopy is the basic tool for studying molecular physics and realizing biochemical sensing. However, it is challenging to realize sub-femtometer resolution spectroscopy over broad bandwidth. Broadband and high-resolution spectroscopy with calibrated optical frequency is demonstrated by bridging the fields of speckle pattern and electro-optic frequency comb. A wavemeter based on a whispering-gallery-mode barcode is proposed to link the frequencies of a probe continuous-wave laser and an ultrastable laser. The ultrafine electro-optic comb lines are generated from the probe laser to record spectrum of sample with sub-femtometer resolution. Measurement bandwidth is a thousandfold broader than comb bandwidth, by sequentially tuning the probe laser while its wavelength is determined. This approach fully exploits the advantages of two fields to realize 0.8-fm resolution with a fiber laser and 80-nm bandwidth with an external cavity diode laser. The spectroscopic measurements of an ultrahigh Q -factor cavity and gas molecular absorption are experimentally demonstrated. The compact system, predominantly constituted by few-gigahertz electronics and telecommunication components, shows enormous potential for practical spectroscopic applications.

Keywords: frequency comb; reconstructive wavemeter; spectroscopy.

Received Aug. 23, 2023; revised manuscript received Dec. 28, 2023; accepted for publication Jan. 11, 2024; published online Feb. 6, 2024.

© The Authors. Published by SPIE and CLP under a Creative Commons Attribution 4.0 International License. Distribution or reproduction of this work in whole or in part requires full attribution of the original publication, including its DOI.

[DOI: [10.1117/1.AP.6.1.016006](https://doi.org/10.1117/1.AP.6.1.016006)]

1 Introduction

Spectroscopy is the essential tool to investigate the structures of atoms and molecules, which has outstandingly contributed to atomic and molecular physics, analytical chemistry, and molecular biology. It also gained enormous significance in the fields of optical sensing, environmental study, and medical diagnostics. High spectral resolution is required in Doppler-free spectroscopy, high- Q cavity characterization, and precise sensing. Broadband spectroscopy with calibrated frequency is vital

for investigations of multiple samples and interrogations of multiplexed sensors.

Spectrometers, widely implemented in spectroscopic measurement, are facilitated by using speckle patterns.^{1,2} The speckle pattern generated in disordered media is unique at each wavelength to reconstruct the input spectrum. Random reflection, scattering, and interference generate speckle patterns during the propagation of light in multimode fiber,^{3–9} single-mode fiber,^{10,11} integrating sphere,¹² integrated waveguide,^{13–15} or more disordered materials.^{16–18} With longer relative optical path length, the compact speckle-based spectrometers with picometer resolution outperform the state-of-the-art grating spectrometers. Combined with optical frequency comb (OFC), a multimode fiber spectrometer performs spectroscopy of acetylene.⁶ Higher resolution can be reached by using a speckle

*Address all correspondence to Xinyu Fan, fan.xinyu@sjtu.edu.cn

[†]These authors contributed equally to this work.

[‡]Present address: Max-Planck Institute of Quantum Optics, Hans-Kopfermann-Straße 1, 85748 Garching, Germany

pattern to determine a single wavelength instead of measuring the spectrum, as does a speckle-based wavemeter. Sub-femtometer resolution has been demonstrated using integrating sphere,¹² multimode fiber,⁷ and fiber Rayleigh scattering.¹¹ Assisted with a convolutional neural network, even two attometers' difference of optical wavelength can be distinguished.⁸ When determining one or few sparse discrete wavelengths, a speckle pattern-based wavemeter is not effective for spectroscopic measurement. Therefore, the potential of speckle patterns in high-resolution spectroscopy still needs to be exploited.

The OFC,^{19,20} invented from the femtosecond pulse laser for optical metrology, has significantly promoted precision spectroscopy by building a link between optical frequency and radio frequency (RF). The equidistant coherent lines of OFC are also powerful tools to measure broadband spectra in direct comb spectroscopy, and line resolving can be performed using virtually imaged phase array,²¹ scanning Fabry–Perot (F–P) cavity,²² Fourier transform spectrometer,²³ heterodyne interferometer,²⁴ and dual-comb spectrometer.²⁵ Advanced comb-based spectroscopy, such as dual-comb spectroscopy, can exploit the frequency resolution, frequency accuracy, and broad bandwidth of OFC.²⁶ The resolution of comb-based spectroscopy is generally equal to the comb repetition rate. Although interleaved frequencies can be sampled by shifting the comb in principle, shifting two mutually coherent comb sources locked to atom clock at fine steps may only be performed in an advanced metrology laboratory.²⁷ Spectroscopic techniques have developed together with the new demonstrations of comb sources in the last decade with different repetition frequencies at more wavelength regions.^{28–30} Compared to most of combs generated from cavities with a physical length limited repetition rate, electro-optic frequency comb (EOFC) has a freely selected repetition rate driven by an RF signal and provides ultrafine comb lines for sub-femtometer resolution spectroscopy.

EOFC can be generated by overdriving modulators using a high-voltage signal for high-order sidebands with a limited number of comb lines.^{30,31} Recent demonstrations using tailored waveforms in electro-optic modulation could cost-effectively generate more comb lines. Tailored waveforms are designed by inverse Fourier transformation of equidistant frequency components, including pseudo-random bit sequence,^{24,32} frequency chirp,^{33,34} pulse,³⁵ or chirped pulse,^{36,37} generated from arbitrary waveform generator, programmable pulse generator, step recovery diode,³⁸ and direct digital synthesizer.³⁹ The repetition rate, depending on repetitive period, easily reaches megahertz, kilohertz or even sub-kilohertz levels.³⁹ For these ultrafine EOFCs, the bandwidths, approximately proportional to repetition rate, are much more limited within electronics bandwidth. Although source lasers provide agility of center wavelength, due to pm precision of laser tuning, the measurement bandwidth of femtometer-resolution EOFC is hardly broadened.⁴⁰ Extending the measurement bandwidth of ultrafine EOFC is attractive in precise spectroscopy and high-sensitivity sensing.

Here, a broadband speckle generated from whispering-gallery-mode (WGM) resonator breaks the bandwidth limitation of sub-femtometer-resolution EOFC to reach the tunable range of the source laser by linking its center frequency to an optical reference. High-resolution spectrum of sample and accurately determined frequency of each comb line are simultaneously obtained in sub-millisecond measurement time. Spectroscopic measurements of a fiber F–P cavity with 0.8 fm resolution and HCN gas cell with 40 nm bandwidth are, respectively,

demonstrated with a fiber laser and an external cavity diode laser (ECDL). Our work leverages the advantages of speckle-based wavemeter and ultrafine EOFC to achieve ultrahigh-resolution spectroscopy with calibrated frequency over a broad bandwidth.

2 Principles and Methods

Long optical path length and random features are expected for speckle-based spectrometer or wavemeter. Among existing structures, WGM resonators have an exceptionally high Q -factor and easily excited multiple modes, which may simultaneously realize high resolution and miniaturization. The WGM barcodes, composed of multiple WGM resonances, are unique at different temperatures and were first proposed for temperature sensing.⁴¹ The WGM barcodes (or WGM speckle patterns) are also unique at each optical frequency (or wavelength), since depths, spacings, linewidths, and resonant wavelengths of WGM resonances are different. Here, a wavelength or optical frequency determination scheme based on WGM barcodes is proposed, which benefits from the crowded WGMs instead of trying to obtain a series of clean single-mode resonances. As shown in Fig. 1, the relative optical frequency of an unknown CW laser can be determined by comparing its individual WGM speckle with a prerecorded reference speckle, due to the relationship between WGM speckle and optical frequency. An ultrastable laser with known frequency f_{ref} provides its WGM speckle to calibrate the frequency of a whole reference speckle. The frequency shift of a WGM speckle introduced by external perturbation, such as temperature variation or vibration, is also eliminated in measurement. As shown in Fig. 1, the reference speckle serves as a broadband and fine “ruler” to determine the calibrated frequency f_1 of the unknown laser. This proposed scheme can independently work as a broadband and high-resolution wavemeter based on a compact WGM resonator. Sub-femtometer resolution over tens of nanometers of bandwidth is realized with a 1.5 mm-diameter microrod resonator. In this paper, it shows potential for spectroscopy in novel combination with an ultrafine EOFC.

An EOFC with arbitrarily selected repetition frequency can be generated from the CW laser. Especially, without physical restriction of cavity length, sub-femtometer-interval comb lines (less than 125 kHz at telecommunication wavelength) are feasible to record ultrahigh resolution spectra of the samples. Accordingly, the bandwidth of such an EOFC is only tens of picometers, due to the universal limitation of the number of comb lines in EOFC generation. Even so, a tunable seed laser can offer the frequency agility (f_2 , f_3 , and f_4 exemplified in Fig. 1) of EOFC to obtain a series of spectra. These resulting spectra can be stitched together if the frequency of the tunable seed laser is accurately determined by the WGM speckle-based wavemeter. With this scheme, the bandwidth of spectroscopic measurement is far extended to the tunable range of laser, which is a thousandfold of the original EOFC bandwidth.

The WGM resonator in our experiment is a fused silica microrod with a diameter of 1.5 mm fabricated by using CO₂ laser. A tapered fiber is used to couple the light into and out of the resonator. The microrod resonator and tapered fiber are attached by using ultraviolet-curing adhesive for long-term stability. Adhesion reduces its Q -factor from 7×10^7 to 1.1×10^7 . The average transmission loss is about 10.2 dB. No transmitted power fluctuation is observed. The input polarization state of the WGM resonator is held using a polarization controller.

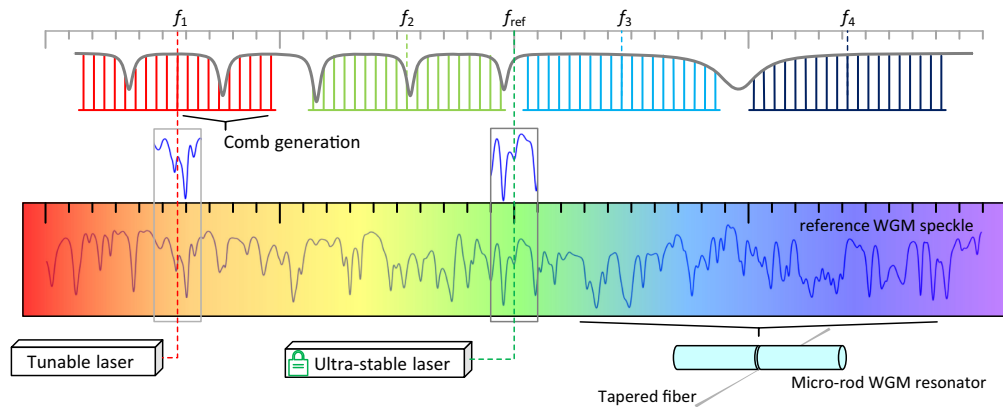


Fig. 1 Speckle-based spectroscopy with an EOFC. Reference WGM speckle, excited from a microrod resonator attached with a tapered fiber, is unique to be a “ruler” to determine the calibrated frequency of probe laser for electro-optic comb generation. The measurement bandwidth of narrowband ultrafine electro-optic comb is unlocked to the range of tunable probe laser while its center frequency is determined. An ultrastable laser for frequency calibration also eliminates external perturbation-induced shift of speckle. Ultrahigh-resolution spectroscopy with far extended bandwidth can be performed.

A specific experimental setup is shown in Fig. 2. The ultra-stable laser is a fiber laser locked to an ultrastable vacuum F–P cavity (provided by Stable Laser Systems) by using Pound–Drever–Hall locking technique. The finesse of cavity is up to 400 k. The nominal daily frequency drift is <100 kHz with actively stabilized temperature, vacuum, and passively isolated vibration. Hence, its optical frequency is regarded to be a constant in experiment. The reference to a metrology frequency comb or an atom resonance, not equipped here, may enable the absolute frequency measurement.

The reference speckle and individual speckle are obtained by an RF-driven swept laser configuration. A linearly frequency swept RF signal with a sweep range of 8 GHz is applied on the single-sideband modulator (SSBM). The modulated laser, passing through the WGM resonator, is detected by a photodetector (PD) with 120 MHz bandwidth. The power fluctuation, caused by modulator frequency response, is eliminated by introducing a branch without a resonator. Only a tunable laser is utilized to prerecord the reference speckle by tuning its center

frequency with a step of about 5 GHz (or 40 pm). The spectra of adjacent acquisitions have an overlapping region for stitching. The stitching points are calculated by using a cross-correlation algorithm. The overall reference speckle in 10 THz bandwidth can be obtained, which is limited by the operation window of the modulators and tunable range of source laser. The tunable laser and the ultrastable laser are used together to obtain measurement speckle for frequency determination. The cross-correlation curve calculated by comparing the measurement speckle and the reference speckle provides two distinguished peaks, representing the frequencies of tunable laser and ultrastable laser, respectively, while the measurement speckle is the superposition of each individual WGM speckle. Therefore, the calibrated frequency of the tunable laser can be derived from the relative peak locations. The calibrated readout prevents the linear drift of WGM speckle introduced by surrounding perturbation.

Another partial output of the tunable laser is modulated by using an electro-optic modulator (EOM) for EOFC generation. The modulator is driven by a tailored waveform designed by

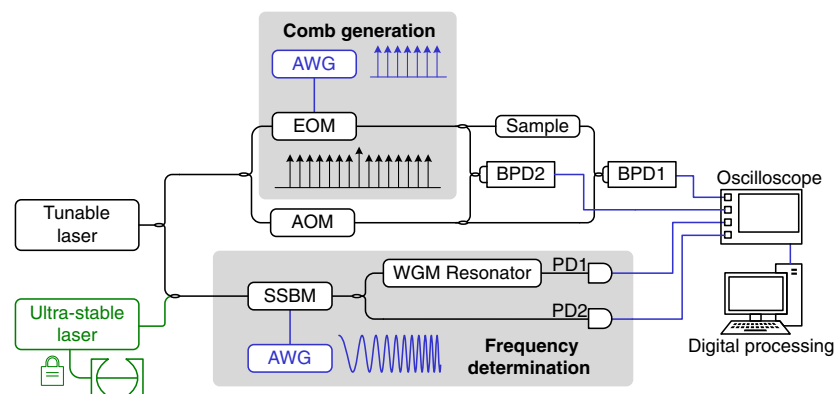


Fig. 2 The experimental setup of the speckle-based spectroscopy with an EOFC. AWG, arbitrary waveform generator; EOM, electro-optic modulator; SSBM, single-sideband modulator; WGM, whispering-gallery-mode; PD, photodetector; BPD, balanced photodetector.

inverse Fourier transformation of multiple frequency components with parabolic phase relation (See Fig. S1 in the [Supplementary Material](#)). The driven signal in the frequency domain already looks like an “electrical comb.” The repetitive period is freely selected, 10 or 1 μ s in our demonstration (corresponding to 100 kHz or 1 MHz repetition rate). The RF bandwidth is 1.5 GHz. All EOFC comb lines are positive/negative first-order sidebands, without sacrifice of optical linewidth. A 14-bit low-noise programmable arbitrary waveform generator works at 5 GSamples/s. A self-heterodyne interferometer is used to resolve the comb lines. A center frequency shift, practically 80 MHz plus a quarter of the repetition frequency, is introduced using an acousto-optic modulator to distinguish the positive and negative sidebands. Single EOFC configuration is used instead of dual-EOFC for spectrum acquisition due to its higher refresh time and lower complexity. The interferograms are detected using a balanced photodetector (BPD) with a bandwidth of 1.6 GHz. A data acquisition board with 3.125 GSamples/s digitizes an output signal of four PDs. The RF generators and acquisition board are synchronized to a 10-MHz oscillation generated from an atomic clock.

The spectra of the comb are obtained by Fourier transformation in digital processing. The spectra of samples are recorded by the ultrafine comb lines and demodulated after being compared with spectra of a branch without a sample. The tunable laser is not tuned during the measurement. The acquisition of WGM speckle and comb spectrum can be realized within 80 μ s at one center frequency. We perform a sequence of acquisitions

by changing the center frequency, with a step of about 2.5 GHz for full coverage of the laser tunable range. In the following experiments, a fiber laser with low-frequency noise and an ECDL with broad tuning range, respectively, serve as the tunable probe laser to reach 100-kHz resolution and 80-nm bandwidth. Moderate bandwidth of ultrafine EOFC simplifies the detection with a self-heterodyne interferogram. Broadband spectroscopic measurement is still achieved with the assistance of WGM speckle-based frequency determination.

3 Results

3.1 High Resolution of the System

A fiber laser serves as the tunable laser in the demonstration of high-resolution measurement. The laser provides ± 20 kHz free-running frequency stability in milliseconds measured from the beat note of two of the same fiber lasers. A trade-off between the stability and tunability exists in most laser systems. The tunable range of the fiber laser is 120 GHz, which limits the bandwidth of reference speckle and spectroscopy. The superposed WGM speckles of the tunable laser and the ultrastable laser in 0.8 ms are shown in Fig. 3(a). The range in optical domain is 8 GHz, which contains more than 200 WGM resonances. The number of excited WGMs is evaluated to be about 1600. These resonances have different depths and widths, as shown in the zoom-in image [Fig. 3(b)] in 50 μ s. The WGM speckles composed of a mass of WGM resonances can be regarded as an approximately stochastic curve and are unique at different wavelengths. Cross-

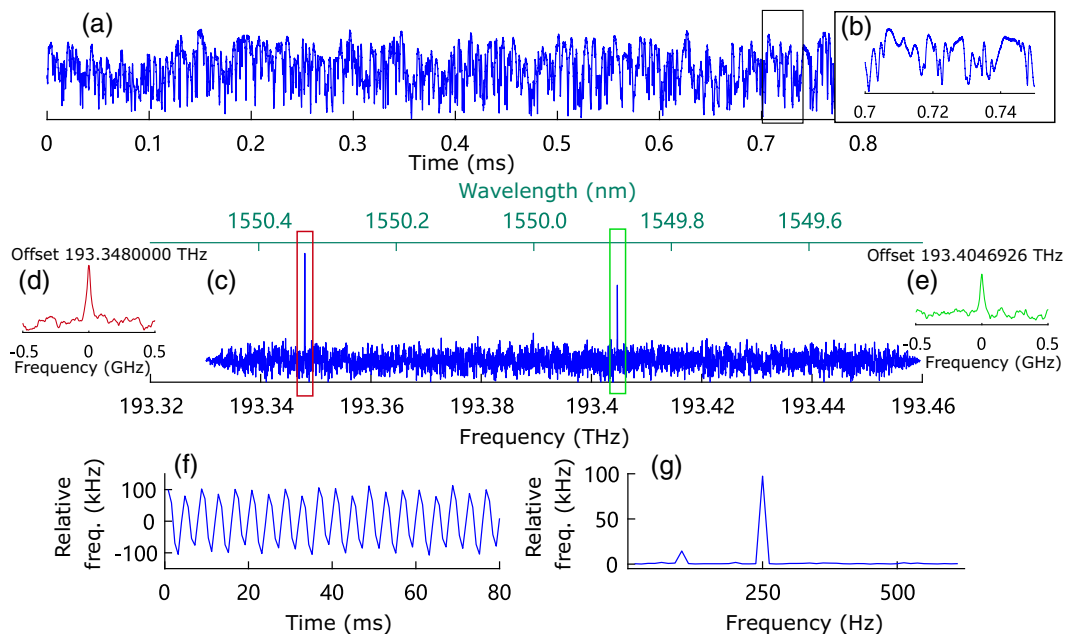


Fig. 3 Frequency determination for a fiber laser with a resolution of 100 kHz in 120 GHz bandwidth. (a) The speckle was recorded in 0.8 ms, corresponding to a frequency range of 8 GHz. (b) A zoom-in figure of (a) in 0.05 ms. (c) Cross-correlation result between the measurement speckle and the reference speckle over a bandwidth of 120 GHz. (d) and (e) are zoom-in correlation peaks of the reference laser and the fiber laser. The frequency of the tunable laser is determined to be 193.4046926 THz. The FWHMs of two peaks are both about 41 MHz. (f) Frequency readouts of the fiber laser with frequency modulation. (g) Fourier transformation of frequency readouts. The amplitude and frequency of the modulation are 100 kHz and 250 Hz, respectively. The sampling rate of the frequency readout is 1.25 kHz.

correlation results comparing this measurement speckle and the reference speckle prerecorded with same fiber laser are shown in Fig. 3(c). The left peak, shown in Fig. 3(d) in red, represents the location of the ultrastable laser at 193.3480000 THz (not absolute frequency, but within 100 kHz stability per day), which calibrates the frequency of all the cross-correlation results. The frequency of the fiber laser is determined to be 193.4046926 THz with a resolution of 100 kHz according to the right peak of the correlation curve, as shown in Fig. 3(e). The peak location is obtained using Lorentz fitting. The FWHMs of two peaks are both about 41 MHz. The FWHM of the correlation function is usually regarded as the spectral resolution of a speckle-based spectrometer,⁵ illustrating about 0.32-pm resolution for a WGM resonator working as a spectrometer. Relatively, the resolution of a speckle-based wavemeter is usually evaluated by measuring the wavelength modulation.¹²

The resolution of frequency determination is evaluated by measuring a frequency-modulated fiber laser. Another AOM is introduced to modulate the center frequency of the probe laser. The readouts of the relative frequency obtained from the WGM speckles are shown in Fig. 3(f). The sinusoidal frequency modulation with an amplitude of 100 kHz is well demodulated. The refresh rate of the frequency determination is 1.25 kHz. The Fourier transformation shown in Fig. 3(g) reveals the modulation frequency at 250 Hz with an SNR of 261.

3.2 Spectroscopic Measurement of a High-Q F-P Cavity

The EOFIC with 100 kHz line spacing and 2.5 GHz bandwidth is generated using a tailored waveform and an electro-optic modulator. The reflectance spectrum of an ultrahigh Q -factor fiber cavity composed of two fiber Bragg gratings is measured. The reflection band is about 60 GHz. The frequency shift introduced by AOM is 80.025 MHz, with a remainder of a quarter of repetition rate, to fold comb lines within RF detection bandwidth. The interferograms [see Fig. S2(a) in the [Supplementary Material](#)] in 1 ms recording time are Fourier-transformed to obtain the RF spectrum [see Fig. S2(b) in the [Supplementary Material](#)]. The optical spectrum, unfolded from the RF spectrum, is shown in Fig. 4(a) in linear scale. About 25,000 comb lines covering a bandwidth of 2.5 GHz are resolved. The center frequency in the optical domain is determined by the WGM speckle of the source laser in 0.8 ms. The measurement speed depends on the readout rate of frequency determination up to 1 kHz. The 25 kHz refresh rate of heterodyne interferometer could enable time-resolved measurement. A zoom-in figure in 2.5 MHz bandwidth is shown in Fig. 4(b), in which the linewidth of the comb line is Fourier-transform-limited to be 1 kHz. The line spacing is 100 kHz, corresponding to the resolution of spectroscopy. One resonance of the fiber cavity is represented in Fig. 4(b). The demodulated reflection spectrum is the maxima of comb lines in Fig. 4(a) dividing these in the reference branch

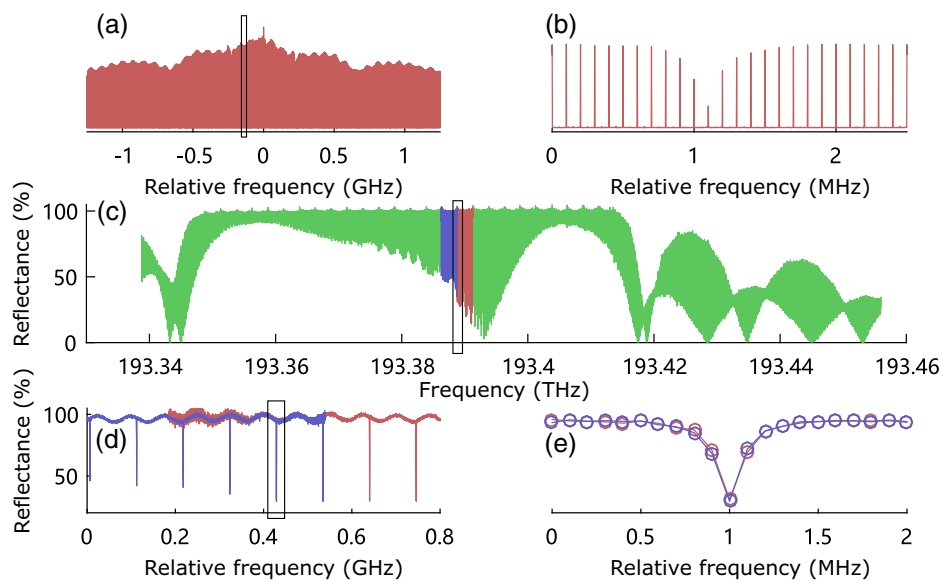


Fig. 4 Spectroscopic measurement of the reflection spectrum of a fiber F-P cavity. (a) Resolved spectrum of the EOFIC in linear scale with a bandwidth of 2.5 GHz by Fourier transformation of data in 1 ms recording time. (b) Zoom-in figure of (a) in the box with resolved comb lines and one recorded resonance. The line spacing, corresponding to the spectral resolution, is 100 kHz. (c) The reflectance spectrum of a fiber F-P cavity in 117 GHz bandwidth. The spectrum is composed of 47 acquisitions by changing the center frequency of the tunable laser. Each acquisition contains 25,000 resolved comb lines with 100 kHz resolution over 2.5 GHz bandwidth. Two acquisitions with adjacent center frequencies are drawn in red and blue. (d) Zoom-in figure of (c) for an overlapped region in 0.8 GHz. The free spectral range of the fiber cavity is measured to be 105.6 MHz. (e) Zoom-in figure of a fiber cavity resonance. The linewidth of the resonance is 250 kHz, corresponding to a Q -factor of 7.7×10^8 . The average SNR is calculated to be 227. It is noted that the SNR of spectra varies based on the intensity of the individual comb lines, and the intensity is not uniform across the spectra.

without a sample. The ratio calculation is for eliminating the unflatness caused by the frequency response of devices.

The spectroscopy with extended bandwidth is performed by adjusting the center frequency of the fiber laser with temperature tuning. At each center wavelength, one acquisition is performed for spectroscopic measurement, and wavelength determination in 1 ms recording time. Each acquisition resolves 25,000 comb lines. All the reflectance spectra in the 117 GHz bandwidth are obtained from a sequence of 47 acquisitions, as shown in Fig. 4(c). The red curve is obtained from Fig. 4(a), and the blue curve is another adjacent channel. Totally $>10^6$ spectral points are demodulated. The cavity resonances are in the reflective band around 193.39 THz in the 60 GHz bandwidth. A portion of two adjacent acquisitions containing several narrow resonances is shown in Fig. 4(d). These resonances in overlapping region are well matched thanks to the frequency calibration. One specific resonance is exemplified in Fig. 4(e). The ripple on the baseline is introduced from the nonresonant reflection in the fiber F-P cavity. The SNR of spectroscopic measurement is 227, calculated from the standard deviation of the baseline, while the ripple is eliminated by using a fitting process in calculation. The free spectral range of the fiber cavity is measured to be 105.6 MHz. The linewidth of the resonance in Fig. 4(e) is 250 kHz, corresponding to a cavity Q -factor of 7.7×10^8 . The ultrahigh- Q cavities, as essential tools in precise optical sensing and nonlinear optics, can be properly characterized with the proposed technique.

3.3 Broad Bandwidth of the System

The broad bandwidth of the system is performed by using an ECDL as the tunable probe laser. The tunable range of the laser

is up to 9.5 THz or 76 nm. The wavelength tuning can be performed manually from the front panel, or by using a programmable software. A LabView-based program automatically controls the laser at sequentially selected wavelengths for reference speckle recording, frequency determination, and spectroscopic measurement. The nominal linewidth of ECDL is about 100 kHz. However, the free-running frequency stability in milliseconds is measured to be ± 0.48 MHz, from the beat note of the ECDL and the fiber laser, which becomes the limitation of spectral resolution. Laser stabilization demonstrated using a speckle-based wavemeter could be introduced to actively suppress the frequency noise and improve the frequency stability for higher resolution measurement.¹² The cross-correlation result between the measurement speckle and prerecorded reference speckle is shown in Fig. 5(a). The measurement time is reduced to 80 μ s for a degraded resolution. The green curve in Fig. 5(b) and the red curve in Fig. 5(c) represent the center frequencies of the ECDL and the ultrastable laser, respectively. The frequency of the ECDL is determined to be 190.164017 THz. The resolution is 1 MHz, limited by the frequency noise of the ECDL rather than instrumental performance.

To evaluate the resolution, frequency modulation with an amplitude of 1 MHz is also introduced by using AOM. The frequency readouts are shown in Fig. 5(d). The measurement rate of the frequency determination is increased to 12.5 kHz. The Fourier transformation reveals the frequency modulation with an amplitude of 1 MHz and a frequency of 2.5 kHz, as shown in Fig. 5(e). Intrinsic frequency noises of the ECDL in the low-frequency region with about 1-MHz amplitudes are also observed. Therefore, the readouts in Fig. 5(d) are the superposition of artificial frequency modulation and the frequency noise of the laser.

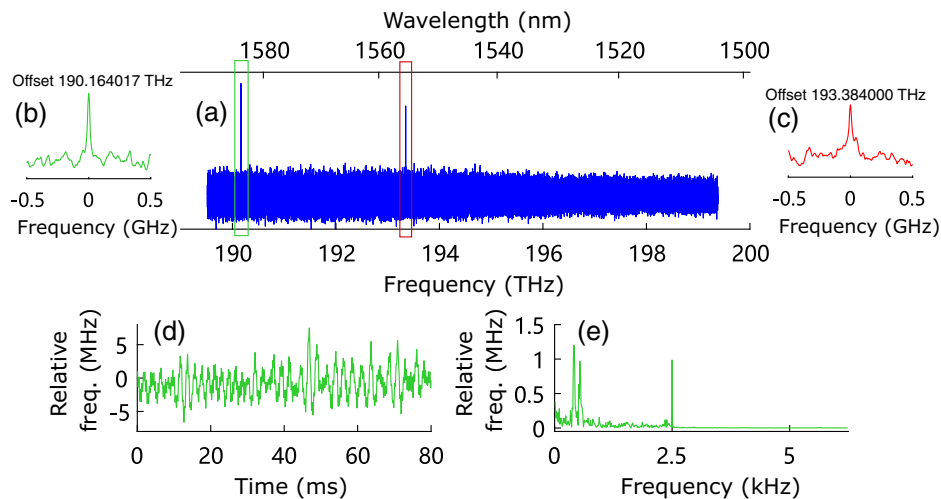


Fig. 5 Frequency determination for the external cavity laser diode with a resolution of 1 MHz in 9.5 THz bandwidth. (a) Cross-correlation result between the measurement speckle and reference speckle over a bandwidth of 9.5 THz. (b) Zoom-in correlation peak of the ECDL. The frequency is determined to be 190.164017 THz. (c) Zoom-in correlation peak of the reference laser. The FWHMs of two peaks are 31 and 54 MHz, respectively. (d) Frequency readouts of the ECDL with frequency modulation. (e) Fourier transformation of (d). The amplitude and frequency of the modulation are 1 MHz and 2.5 kHz, respectively. The low-frequency region is the frequency noise of the ECDL. The averaged frequency error of ECDL in 1 ms (recording time for following spectroscopy experiment) is 0.48 MHz. The sampling rate of frequency determination is 12.5 kHz.

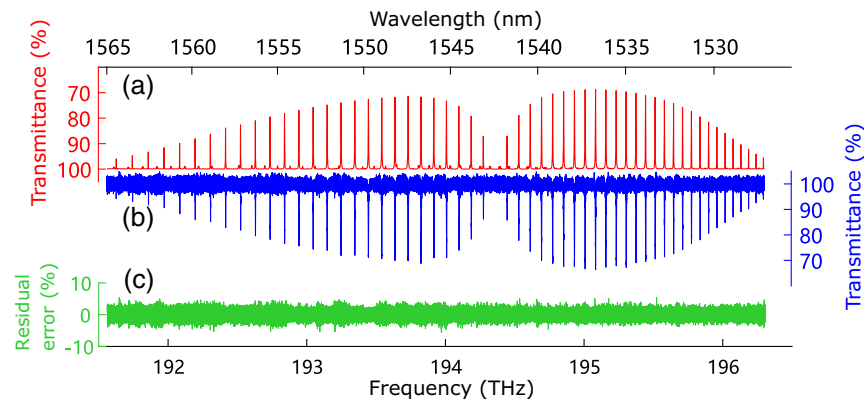


Fig. 6 Spectroscopic measurement of the transmission spectrum of HCN gas cell with 1 MHz resolution. (a) The reference database and (b) the measurement result of HCN transmittance spectrum in 4.74 THz bandwidth (corresponding to 38 nm) with a resolution of 1 MHz. The result is composed of 1890 acquisitions. Each acquisition contains 2350 resolved comb lines with a line spacing of 1 MHz in 1 ms recording time. (c) Residual error between (a) and (b). The standard deviation is 0.0069, corresponding to an SNR of 144.

3.4 Spectroscopic Measurement of HCN Gas

An EOFC with 2.35-GHz bandwidth and 1-MHz repetition rate is generated to measure the transmission spectrum of a H^{13}CN gas cell. The H^{13}CN gas cell with a length of 15 cm and a pressure of 25 Torr is at a laboratory temperature of about 297 K. The wavelength of ECDL is tuned to automatically step using a program. The precision of wavelength tuning is about ± 1 pm (125 MHz), and precise wavelength tuning is not required. The wavelength is kept in 100 μs for frequency determination and spectroscopic measurement, corresponding to a measurement rate of 10 kHz. The results shown in Fig. 6(b) are composed of the resolved spectra of 1890 acquisitions, each acquisition obtained in 100 μs , corresponding to a total measurement time of 0.19 s. The practical wavelength tuning process of ECDL needs 150 ms to reach a steady state of built-in feedback loop. About 7-min of experimental time is required to finish the data recording in Fig. 6(b). Any position within 80 nm bandwidth can be quickly reached by ECDL with 100 nm/s tuning speed. Quickly tuning the laser at non-neighboring wavelength for sparsely distributed features or sensors is also feasible.

Each acquisition at a wavelength contains 2350 comb lines with a resolution of 1 MHz. Totally, 4×10^6 spectral points are resolved in the whole spectrum, covering a bandwidth of 4.74 THz or 38 nm. The measurement result and a reference database of the *R* and *P* branches of H^{13}CN are reversely shown in Figs. 6(b) and 6(a), respectively, in blue and red. The residual errors between the database and the result are shown in Fig. 6(c). The standard deviation is calculated to be 0.69%, corresponding to an SNR of 144.

4 Long-Term Stability

Although the WGM resonator is affected by surrounding temperature and vibration and looks easy to be disturbed, our system shows remarkable robustness in long-term measurement. The microrod resonator and tapered fiber are attached by using ultraviolet-curing adhesive. Adhesion prevents moderate change of coupling states. No transmitted power fluctuation is observed. The nonlinear response of input power can be ignored for a

steady optical power. Other disturbing effects can be categorized into two aspects. One introduces linear frequency shift into the WGM speckle and measurement offset error. Another one distorts the WGM speckle and decreases the cross-correlation coefficient, including the change of linewidth, depth, and the nonlinear frequency shift. The main reason for the former disturbing effect is system linear response of environmental temperature change, which makes the WGM speckle shift in the frequency domain. The distortion of the WGM speckle in the latter aspect is typically caused by change of coupling state, polarization, and nonlinear environmental perturbation. The effect of these perturbations is ultimately reflected in the changes in free spectral range and the *Q*-factor of the WGM speckle. Since the frequency shift of resonance is real-time-calibrated by using a stable reference laser in the experiment, measurement offset error caused by the linear frequency shift can be real-time-eliminated in experiments. However, the distortion of WGM speckle cannot be eliminated. We experimentally monitor the stability of the proposed WGM resonator-based system in 10 h. The change of peak position in the cross-correlation curve indicates measurement offset error caused by the WGM speckle shift, and its coefficient represents the degree of WGM speckle distortion. The evolution of a selected resonance in reference speckle circled in Fig. 7(b) is shown in Fig. 7(a). Its center frequency shift is calibrated by a stable laser. The frequency bias for calibration is within ± 50 MHz, as shown in Fig. 7(c). The change of linewidth is $< \pm 3$ MHz. The calibration process makes the system resistant to linear external perturbation. Two individual speckles are generally considered uncorrelated with correlation coefficient below 0.5. To ensure the accuracy of reconstruction, the correlation coefficient between the distorted WGM speckle and the original WGM speckle should be > 0.5 . The cross-correlation coefficients in 10 h are always above 0.64, as shown in Fig. 7(d), which enables accurate demodulation. Although the resistance of natural external perturbation is observed, it is better to place the cavity in a stable environment in practical measurement and perform reference speckle recording before precise spectroscopy.

We further perform a simulation to quantitatively analyze the effects of the *Q*-factor and free spectral range. The simulated

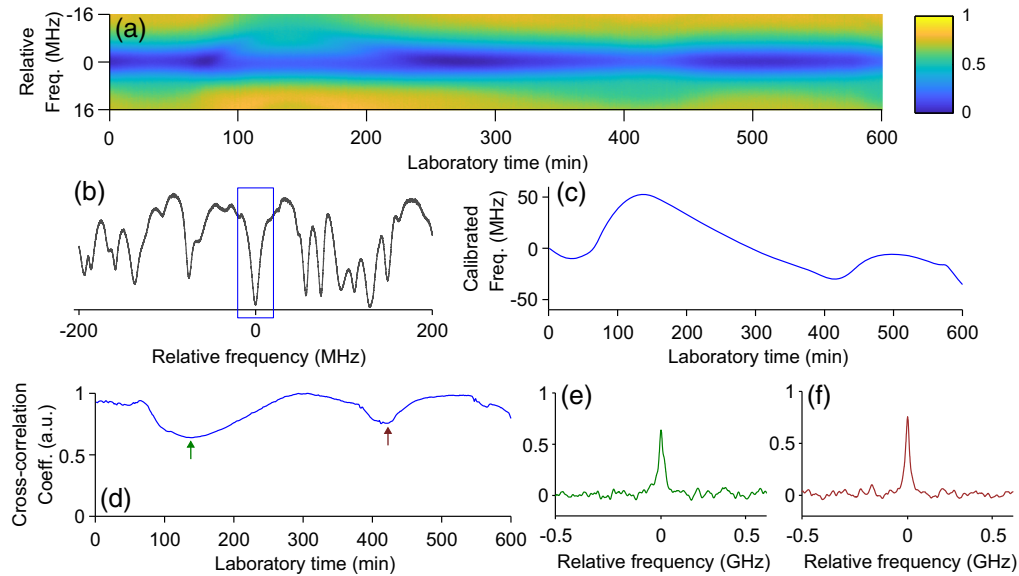


Fig. 7 Long-term stability of WGM resonance and WGM-based wavemeter in 10 h. (a) Linewidth, depth, and center frequency evolution of the WGM resonance circled in (b). (b) A portion of WGM speckle. (c) Frequency bias obtained from the readout of stable laser for calibration. (d) Cross-correlation coefficients, which are always >0.64 . (e) and (f) Cross-correlation peaks pointed by arrows in (d).

result is shown in Fig. 8 (see Fig. S9 in the [Supplementary Material](#) for specific simulated speckles). According to our fabrication and measurement, the initial situation of the cavity is on the top-left corner (Q -factor = 10^7 , and free spectral range = 0.35 nm). The Q -factor and free spectral range are changed to obtain distorted WGM speckle. The cross-correlation between distorted WGM speckle and reference speckle is performed to evaluate the effect of distortion on reconstruction result. The contour line in red illustrates the quantitative bound, where the correlation coefficient is 0.5. The correlation coefficient is above 0.5 within the region, where the Q -factor is $>7.2 \times 10^5$, and the free spectral range change is <12 kHz.

5 Discussion

Optical path length in a speckle-based spectrometer or wavemeter is longer than in conventional spectrum analyzers. WGM resonators have an exceptionally high Q -factor compared to existing structures, which makes high resolution and miniaturization possible. The WGM resonator in our demonstration with sub-femtometer resolution in wavemeter or possibly sub-pm resolution in spectrometer is attractive with a millimeter-scale footprint. Considering inverse relationship between correlation peak FWHM, linking to frequency resolution, and resonator Q -factor is found in our simulation (see Fig. S6 in

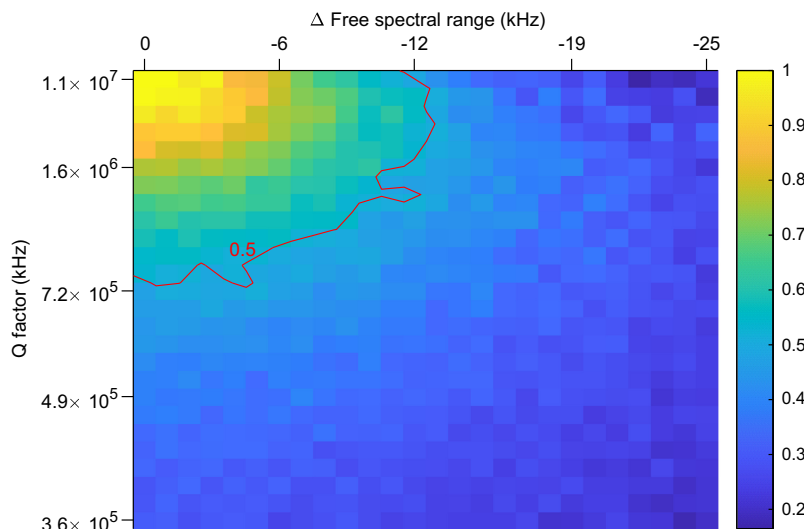


Fig. 8 Cross-correlation coefficient versus the change of Q -factor and free spectral range in simulation. The quantitative bound is illustrated in red, where the correlation coefficient is 0.5.

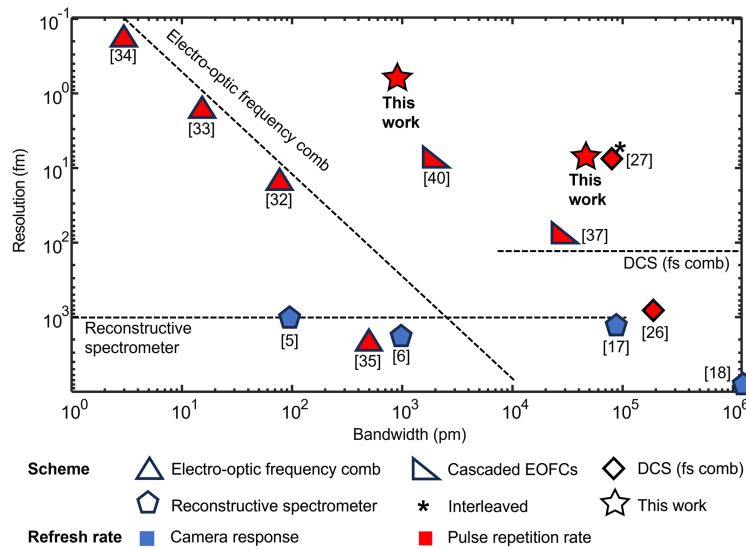


Fig. 9 Performance metric chart of various spectroscopic methods – EOFC, dual-comb spectroscopy, reconstructive spectrometers – using resolution and bandwidth constraints.

the [Supplementary Material](#)), higher resolution may be realized with a billion Q -factor WGM resonator.⁴² In addition, integrated WGM resonators on chip,^{43,44} together with recently developed integrated thin-film lithium niobate and electro-optic comb source,^{45,46} show the potential of a fully integrated system with a smaller footprint.

The operation bandwidths of our demonstration and most EOFC demonstrations are at the telecommunication band. In fact, electro-optic modulators working on almost all near-infrared band are commercially available, supporting the EOFC generation from 800 nm³⁴ to 2 μ m.⁴⁷ Besides, EOFCs at visible, near-ultraviolet and mid-infrared region have been demonstrated via nonlinear frequency conversion.^{48,49} Considering the achievable range of the WGM resonator, we believe the proposed scheme is possible to be extended to all these wavelength regions.

It is instructive to compare the performance of the proposed system with existing various spectroscopic measurement approaches, as shown in Fig. 9, which shows resolution, bandwidth, and measurement speed of selected representative spectroscopic methods. The proposed method combining EOFC and WGM speckle provides 8 fm spectral resolution with 80 nm bandwidth, comparable to interleaved fs-comb-based DCS. Remarkably, another demonstration of 0.8 fm resolution by the proposed scheme outperforms existing methods in bandwidth. Moreover, compared with other spectroscopic methods, the proposed system shows fine stability, a fast refresh rate, low complexity, and much cost-effectiveness (see detailed discussion in the [Supplementary Material](#)).

6 Conclusion

Here, spectroscopic measurement is experimentally demonstrated with a combination of ultrafine EOFC and speckle pattern. The combination fully exploits the high resolution and broad bandwidth property of the speckle-based wavemeter and breaks through the bandwidth limitation of the ultrafine EOFC. Few-gigahertz electronics and telecommunication components are predominantly used in the proposed scheme. The compact

and cost-effective system with high resolution and broad bandwidth will be a prospective way toward precise investigation in biochemical sensing and physics.

Code and Data Availability

The data that support the findings of this study are available from the corresponding author upon reasonable request.

Acknowledgments

We thank Prof. Yuejian Song and Dr. Jun Li from Nanjing University for the fabrication of the resonator. This work is financially supported by the National Natural Science Foundation of China (NSFC) (Grant No. 62275151). The authors declare no conflicts of interest.

References

1. H. Cao and Y. Eliezer, “Harnessing disorder for photonic device applications,” *Appl. Phys. Rev.* **9**(1), 011309 (2022).
2. Y. Wan, X. Fan, and Z. He, “Review on speckle-based spectrum analyzer,” *Photonic Sens.* **11**(2), 187–202 (2021).
3. B. Redding and H. Cao, “Using a multimode fiber as a high-resolution, low-loss spectrometer,” *Opt. Lett.* **37**(16), 3384–3386 (2012).
4. B. Redding, S. M. Popoff, and H. Cao, “All-fiber spectrometer based on speckle pattern reconstruction,” *Opt. Express* **21**(5), 6584–6600 (2013).
5. B. Redding et al., “High-resolution and broadband all-fiber spectrometers,” *Optica* **1**(3), 175–180 (2014).
6. N. Coluccelli et al., “The optical frequency comb fibre spectrometer,” *Nat. Commun.* **7**(1), 12995 (2016).
7. G. D. Bruce et al., “Overcoming the speckle correlation limit to achieve a fiber wavemeter with attometer resolution,” *Opt. Lett.* **44**(6), 1367–1370 (2019).
8. R. K. Gupta et al., “Deep learning enabled laser speckle wavemeter with a high dynamic range,” *Laser Photonics Rev.* **14**(9), 2000120 (2020).
9. T. Wang et al., “High-resolution wavemeter based on polarization modulation of fiber speckles,” *APL Photonics* **5**(12), 126101 (2020).

10. Z. Zhang et al., "A novel wavemeter with 64 attometer spectral resolution based on Rayleigh speckle obtained from single-mode fiber," *J. Lightwave Technol.* **38**(16), 4548–4554 (2020).
11. Y. Wan et al., "Wavemeter capable of simultaneously achieving ultra-high resolution and broad bandwidth by using Rayleigh speckle from single mode fiber," *J. Lightwave Technol.* **39**(7), 2223–2229 (2021).
12. N. K. Metzger et al., "Harnessing speckle for a sub-femtometre resolved broadband wavemeter and laser stabilization," *Nat. Commun.* **8**(1), 15610 (2017).
13. B. Redding et al., "Evanescently coupled multimode spiral spectrometer," *Optica* **3**(9), 956–962 (2016).
14. D. Yi et al., "Integrated multimode waveguide with photonic lantern for speckle spectroscopy," *IEEE J. Quantum Electron.* **57**(1), 0600108 (2020).
15. Z. Zhang et al., "Compact high resolution speckle spectrometer by using linear coherent integrated network on silicon nitride platform at 776 nm," *Laser Photonics Rev.* **15**(11), 2100039 (2021).
16. Y. Kwak et al., "A pearl spectrometer," *Nano Lett.* **21**(2), 921–930 (2020).
17. Q. Cen et al., "Microtaper leaky-mode spectrometer with picometer resolution," *eLight* **3**(1), 9 (2023).
18. N. H. Wan et al., "High-resolution optical spectroscopy using multimode interference in a compact tapered fibre," *Nat. Commun.* **6**(1), 7762 (2015).
19. T. Udem, R. Holzwarth, and T. W. Hänsch, "Optical frequency metrology," *Nature* **416**(6877), 233–237 (2002).
20. S. A. Diddams, "The evolving optical frequency comb," *J. Opt. Soc. Am. B* **27**(11), B51–B62 (2010).
21. S. A. Diddams, L. Hollberg, and V. Mbele, "Molecular fingerprinting with the resolved modes of a femtosecond laser frequency comb," *Nature* **445**(7128), 627–630 (2007).
22. C. Gohle et al., "Frequency comb Vernier spectroscopy for broadband, high-resolution, high-sensitivity absorption and dispersion spectra," *Phys. Rev. Lett.* **99**(26), 263902 (2007).
23. J. Mandon, G. Guelachvili, and N. Picqué, "Fourier transform spectroscopy with a laser frequency comb," *Nat. Photonics* **3**(2), 99–102 (2009).
24. N. B. Hébert et al., "Self-heterodyne interference spectroscopy using a comb generated by pseudo-random modulation," *Opt. Express* **23**(21), 27806–27818 (2015).
25. I. Coddington, N. Newbury, and W. Swann, "Dual-comb spectroscopy," *Optica* **3**(4), 414–426 (2016).
26. I. Coddington, W. C. Swann, and N. R. Newbury, "Coherent multiheterodyne spectroscopy using stabilized optical frequency combs," *Phys. Rev. Lett.* **100**(1), 013902 (2008).
27. S. A. Meek et al., "Doppler-free Fourier transform spectroscopy," *Opt. Lett.* **43**(1), 162–165 (2018).
28. T. J. Kippenberg et al., "Dissipative Kerr solitons in optical microresonators," *Science* **361**(6402), eaan8083 (2018).
29. A. Hugi et al., "Mid-infrared frequency comb based on a quantum cascade laser," *Nature* **492**(7428), 229–233 (2012).
30. A. Parriaux, K. Hammani, and G. Millot, "Electro-optic frequency combs," *Adv. Opt. Photonics* **12**(1), 223–287 (2020).
31. B. Xu et al., "Sub-femtometer-resolution absolute spectroscopy with sweeping electro-optic combs," *Opto-Electron. Adv.* **5**(12), 210023 (2022).
32. Y. Bao et al., "A digitally generated ultrafine optical frequency comb for spectral measurements with 0.01-pm resolution and 0.7- μ s response time," *Light Sci. Appl.* **4**(6), e300 (2015).
33. D. A. Long et al., "Multiplexed sub-Doppler spectroscopy with an optical frequency comb," *Phys. Rev. A* **94**(6), 061801 (2016).
34. D. A. Long et al., "Electromagnetically induced transparency in vacuum and buffer gas potassium cells probed via electro-optic frequency combs," *Opt. Lett.* **42**(21), 4430–4433 (2017).
35. G. Millot et al., "Frequency-agile dual-comb spectroscopy," *Nat. Photonics* **10**(1), 27–30 (2016).
36. S. Wang et al., "Fast mhz spectral-resolution dual-comb spectroscopy with electro-optic modulators," *Opt. Lett.* **44**(1), 65–68 (2019).
37. B. Xu et al., "Broadband and high-resolution electro-optic dual-comb interferometer with frequency agility," *Opt. Express* **27**(6), 9266–9275 (2019).
38. A. J. Fleisher et al., "Coherent cavity-enhanced dual-comb spectroscopy," *Opt. Express* **24**(10), 10424–10434 (2016).
39. D. A. Long and B. J. Reschovsky, "Electro-optic frequency combs generated via direct digital synthesis applied to sub-doppler spectroscopy," *OSA Contin.* **2**(12), 3576–3583 (2019).
40. B. Xu et al., "Wideband and high-resolution spectroscopy based on an ultra-fine electro-optic frequency comb with seed lightwave selection via injection locking," *Opt. Lett.* **46**(8), 1876–1879 (2021).
41. J. Liao and L. Yang, "Optical whispering-gallery mode barcodes for high-precision and wide-range temperature measurements," *Light Sci. Appl.* **10**(1), 32 (2021).
42. A. Shitikov et al., "Billion Q -factor in silicon WGM resonators," *Optica* **5**(12), 1525–1528 (2018).
43. C. Wang et al., "High- Q microresonators on 4h-silicon-carbide-on-insulator platform for nonlinear photonics," *Light Sci. Appl.* **10**(1), 139 (2021).
44. Q. Luo et al., "Microdisk lasers on an erbium-doped lithium-niobate chip," *Sci. China Phys. Mech. Astron.* **64**(3), 234263 (2021).
45. D. Zhu et al., "Integrated photonics on thin-film lithium niobate," *Adv. Opt. Photonics* **13**(2), 242–352 (2021).
46. M. Yu et al., "Integrated femtosecond pulse generator on thin-film lithium niobate," *Nature* **612**(7939), 252–258 (2022).
47. A. Parriaux, K. Hammani, and G. Millot, "Electro-optic dual-comb spectrometer in the thulium amplification band for gas sensing applications," *Opt. Lett.* **44**(17), 4335–4338 (2019).
48. B. Xu, T. W. Hänsch, and N. Picqué, "Near-ultraviolet dual-comb spectroscopy with photon-counting," in *CLEO: Sci. and Innov.*, Optica Publishing Group, p. SM1D-4 (2022).
49. M. Yan et al., "Mid-infrared dual-comb spectroscopy with electro-optic modulators," *Light Sci. Appl.* **6**(10), e17076 (2017).

Bingxin Xu is currently a postdoctoral researcher at Max-Planck Institute of Quantum Optics, Germany. He received his PhD in electronics engineering from Shanghai Jiao Tong University in 2021. His research interests are dual-comb spectroscopy, electro-optic frequency comb, optical sampling, and reconstructive spectrometer.

Yangyang Wan received his PhD from Shanghai Jiao Tong University, Shanghai, China, in 2023. He received his BS degree from Huazhong University of Science and Technology, Wuhan, China. He is currently a postdoctoral researcher at the Center for Intelligent Photonics, Shanghai Jiao Tong University, Shanghai, China. His research interests include spectrum measurement, distributed optical fiber sensing, and machine learning.

Xinyu Fan received his BS and MS degrees in applied physics from Shanghai Jiao Tong University in 2000 and 2003, respectively, and his PhD in electrical engineering from the University of Tokyo in 2006. He joined NTT Access Network Service Systems Laboratories in 2006, where he researched on optical reflectometry and optical measurement. Since 2012, he has been in the Department of Electronic Engineering, Shanghai Jiao Tong University, where he is currently a professor. His research interests include distributed fiber-optic sensing, dual-comb spectroscopy, and optical precision measurement technology.

Zuyuan He received his BS and MS degrees in electronic engineering from Shanghai Jiao Tong University in 1984 and 1987, respectively,

and his PhD in optoelectronics from the University of Tokyo in 1999. He joined Nanjing University of Science and Technology as a research associate in 1987, and became a lecturer in 1990. From 1995, he was a research fellow and later a research associate at the University of Tokyo. In 2001, he joined CIENA Corporation as a lead engineer. He returned to the University of Tokyo as a lecturer in 2003, and became an

associate professor in 2005, and a full professor in 2010. He is currently a chair professor and the director of the State Key Laboratory of Advanced Optical Communication Systems and Networks, Shanghai Jiao Tong University. His current research interests include optical fiber sensors, specialty optical fibers, and optical inter-connection.